Annals of Nuclear Medicine Vol. 5, No. 4, 139–144, 1991

Experimental analysis of scattered photons in Tc-99m imaging with a gamma camera

Akihiro KOJIMA,* Masanori MATSUMOTO** and Mutsumasa TAKAHASHI*

*Department of Radiology, Kumamoto University School of Medicine
**Department of Radiological Technology, College of Science, Kumamoto University

The amount of scattered photons in a clinical imaging window of Tc-99m was experimentally measured by means of a line source with scattering materials and a gamma camera. A symmetrical photopeak energy window centered at 140 keV with a width of 20% (126–154 keV) was partitioned into several small windows. Energy spectra were analyzed to determine the scatter fraction and the attenuation coefficient for each window. Line spread functions (LSF) were also obtained to characterize the spatial scatter distribution. The results of analysis of energy spectra show that scattered photons are included over the symmetric 20% window (SW) and scatter fractions increase linearly with the increasing thickness of the scattering material in all energy windows investigated. In addition, the results for the LSF show that the scatter distribution within the SW is represented as a mono-exponential function. Experimental measurements obtained with a phantom and a gamma camera simplify accurate quantification of scattered photons. Such quantitative analysis of scattered photons is important in developing and evaluating a scatter correction technique.

Key words: Compton scatter, attenuation coefficient, scatter fraction, line spread function

INTRODUCTION

A CONVENTIONAL ENERGY WINDOW USED for nuclear medicine imaging contains not only primary photons but also photons scattered within a body because of the limited energy resolution of a gamma camera. In single photon emission computed tomography (SPECT), scattered photons are in the order of 30% to 60% of primary photons within such an energy window.[1,2] Since these scattered photons give false positional information, the acquired images are degraded and accurate quantification of radioactivity in the body is inhibited. Therefore, in order to correct such scattered photons, several methods have been proposed for SPECT.[3–5]

Energy spectra and spatial distributions of photons are often used to develop a new scatter correction technique and evaluate the proposed one. Such information can be obtained by Monte Carlo simulations and experimental measurements. The Monte Carlo technique can discriminate scattered photons from primary ones.[1,2,6,7] However, a typical Monte Carlo calculation is time consuming and cannot perfectly simulate various imaging parameters. On the other hand, the experimental measurements can practically and accurately provide energy spectra and images by means of a phantom and a gamma camera. Therefore, in order to investigate the amount of scattered photons within a clinically used energy window, we experimentally obtained energy spectra and images for a line source and analyzed them quantitatively.

The purpose of this work is to determine the scatter fraction (the ratio of scattered to non-scattered photons), the attenuation coefficient and the spatial distribution of scattered photons within a 20% symmetrical energy window centered at the photopeak of Tc-99m (140 keV), by varying the thickness of the scattering material.

Received May 29, 1991, revision accepted August 21, 1991.

For reprints contact: Akihiro Kojima, M.Sc., Department of Radiology, Kumamoto University School of Medicine, 1-1-1, Honjo, Kumamoto 860, JAPAN.

MATERIALS AND METHODS

Equipment

A gamma camera (GCA-10A, Toshiba, JAPAN) was used with a low-energy, parallel-hole, general purpose collimator. Energy signals which summed up all 37 photomultiplier tubes of the gamma camera were recorded with a multichannel analyzer (Series 30, Canberra, U.S.A.). Each energy spectrum was obtained in the 1 keV/channel. The energy resolution of the camera was 12% for 140 keV and the field of view of the camera was 25 cm. The scintillator thickness was 9 mm.

Measurement of energy spectra

A vinyl plastic tube (1 mm in diameter, 10 cm in length) filled with a solution of Tc-99m (50 MBq) was used as a line source and the acrylic plates (each 30 cm × 30 cm × 2 cm-thick) were employed as uniform scattering materials. The line source was placed 20 cm from and parallel to the collimator face at the center of the acrylic plates. Energy spectra were measured for two kinds of scatter: backscatter and forward scatter. For the backscatter alone a 10 cm thick acrylic plate was used. For the forward scatter alone the acrylic plates were set on the line source with the thickness changed from 0 to 20 cm in 2 cm increments (Fig. 1). All data were corrected for the time decay of Tc-99m.

Analysis of energy spectra

From the energy spectrum data for the forward scatter, the attenuation coefficient was calculated at each energy in the photopeak window by means of the following equation;

$$\mu_d(E)=1/d \cdot \ln[C_0(E)/C(E)] \quad (1)$$

where $C(E)$ and $C_0(E)$ are the counts at energy E with and without scattering material of thickness d, respectively.

The following energy windows around the photopeak of Tc-99m were considered and the counts in these energy windows were integrated: (a) WL1, 126–132 keV; (b) WL2, 133–139 keV; (c) WH1, 140–146 keV; (d) WH2, 147–153 keV; (e) WL, 126–139 keV; (f) WH, 140–153 keV. Furthermore, the total counts in the symmetrical window SW (140 keV ± 10%; 126–153 keV) and the asymmetric window ASW (140 keV −5% to +10%; 133–153 keV), used in clinical imaging of Tc-99m, were also obtained. These counts were represented as a function of energy window w and thickness d by means of

$$T(w, d)=S(w, d)+D(w, d) \quad (2)$$

where $S(w, d)$ is the count for scattered photons and $D(w, d)$ is the count for non-scattered photons. Using the theoretical linear attenuation coefficient μ_a and $S(w, 0)=0$, the $D(w, d)$ can be given by,

$$D(w, d)=D(w, 0) \exp(-\mu_a d)$$
$$=T(w, 0) \exp(-\mu_a d) \quad (3)$$

Therefore, the scatter fraction, defined as the ratio of scattered to non-scattered counts, was obtained as the following equation;

$$SF=\frac{S(w, d)}{D(w, d)}=\frac{T(w, d)-D(w, d)}{D(w, d)}$$
$$=\frac{T(w, d)}{T(w, 0)} \exp(\mu_a d)-1 \quad (4)$$

In addition, the linear attenuation coefficient was calculated by means of the following equation;

$$\mu_w(d)=1/d \cdot \ln[T(w, 0)/T(w, d)] \quad (5)$$

As a result, a relationship between the energy E and the linear attenuation coefficient $\mu_d(E)$ was obtained for various thicknesses of the scattering material. In addition, the total count $T(w, d)$, the scatter fraction SF and the linear attenuation coefficient $\mu_w(d)$ were obtained as a function of the thickness of the scattering material for all energy windows investigated.

Imaging of a line source

To investigate the spatial distribution of scattered photons, three line source images were obtained with three energy windows (WL, WH, and SW) for the

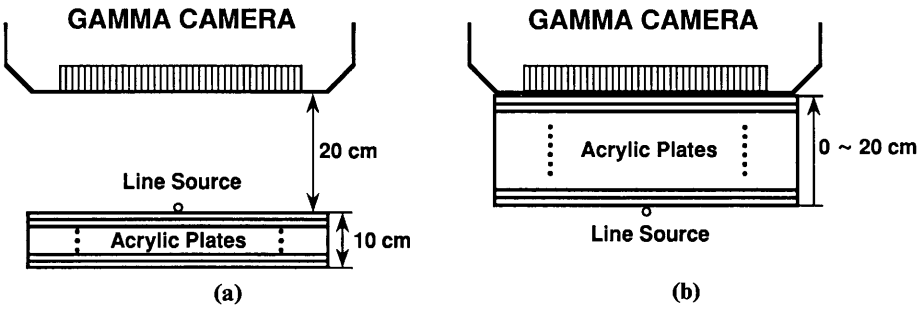

Fig. 1 Experimental diagram for measurements of energy spectra and images: (a) with backscattering material, (b) with forward scattering material.

forward 10 cm scattering material. As a reference image, an image of the line source was also obtained with the SW in air. The line source was kept 10 cm from the collimator face. The matrix size was 256× 256 and one pixel size was 1 mm. The acquisition counts were about one million counts for these images. Then, as the uniformity of the gamma camera sensitivity was degraded due to the asymmetry of the energy windows, uniformity corrections of these images were performed with the flood data (50 million counts) collected within the same energy windows. Profile curves with a seven-pixel width were obtained through the center of each image as the line spread functions.

RESULTS

The energy spectra obtained with backscatter alone and without the scattering material are shown in Fig. 2. The data show that backscattering occurs below 120 keV, while the photopeak is identical in both energy spectra.

Figure 3 shows the energy spectra for forward scattering materials with the thickness ranging from 0 to 20 cm. As the scattering material thickness increased, the maximum value for the photopeak moved to lower energies because of increased inclusion of scattered photons within the photopeak. For the 10 cm thickness, there was a 3 keV shift in the peak position.

Figure 4 indicates the attenuation coefficient calculated by means of Eq. 1 in the photopeak window. Although the attenuation coefficients were affected by the thickness of the scattering material below 140 keV, they were almost constant above 140 keV. Table 1 lists the mean and standard deviation (S.D.)

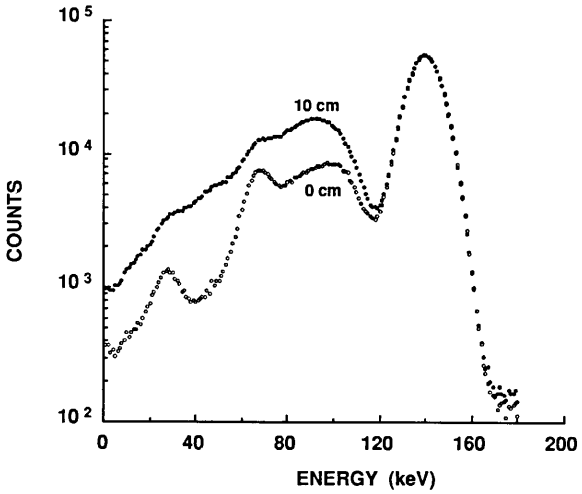

Fig. 2 Energy spectra with and without backscattering material. The thickness of the scattering material was 10 cm.

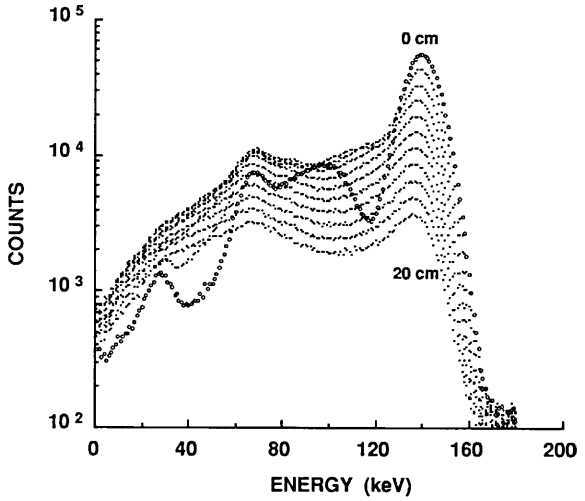

Fig. 3 Energy spectra with and without forward scattering materials. The thickness of materials was changed from 2 to 20 cm in 2 cm increments.

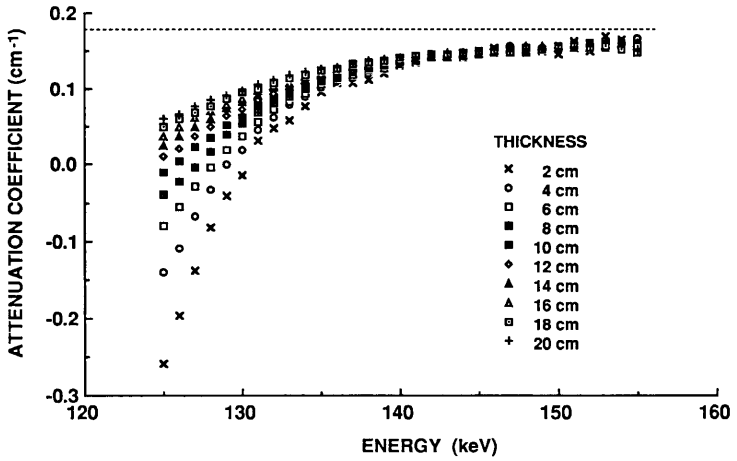

Fig. 4 Attenuation coefficient calculated within energy window 140 keV±10% for various thicknesses of forward scattering materials. The broken line shows the theoretical value (0.178 cm^{-1}).

Table 1 Attenuation coefficients at three energies

	Energy (keV)		
	140	145	150
Attenuation coefficient mean±S.D. (cm^{-1})	0.137 ±0.0036	0.148 ±0.0015	0.153 ±0.0029

S.D.: standard deviation

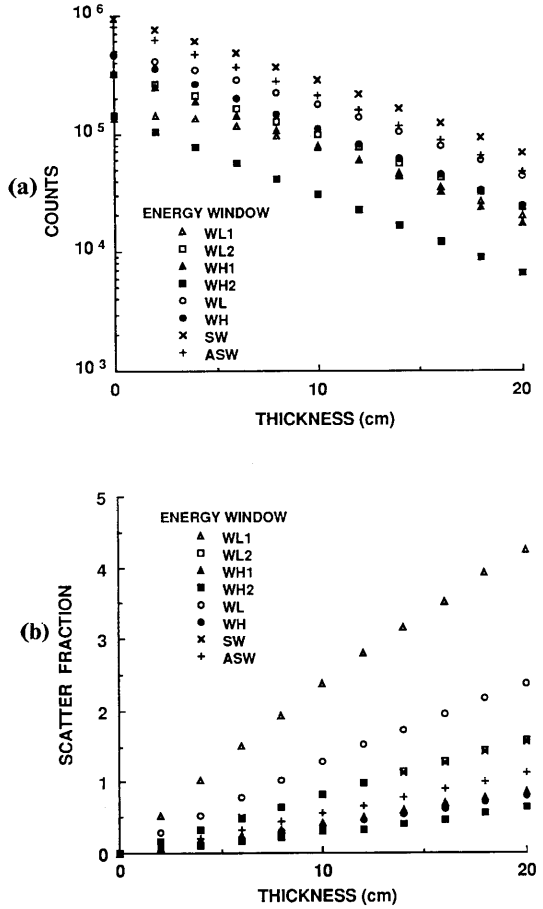

Fig. 5 Counts (a) and scatter fractions (b) as a function of thickness for various energy windows; WL1: 126–132 keV, WL2: 133–139 keV, WH1: 140–146 keV, WH2: 147–153 keV, WL: 126–139 keV, WH: 140–153 keV, SW: 126–153 keV, and ASW: 133–153 keV.

of the attenuation coefficient at 140, 145 and 150 keV. As the energy increased, the attenuation coefficient was closer to the theoretical value (0.178 cm^{-1} from reference[8]). The larger S.D. at 150 keV was due to the low count statistics.

The total counts and the scatter fractions plotted against the thickness of the scattering material for various energy windows are shown in Fig. 5. From Fig. 5a it was seen that although there were shoulder regions at the thinner scattering material thickness in every window below 140 keV (WL1, WL2 and

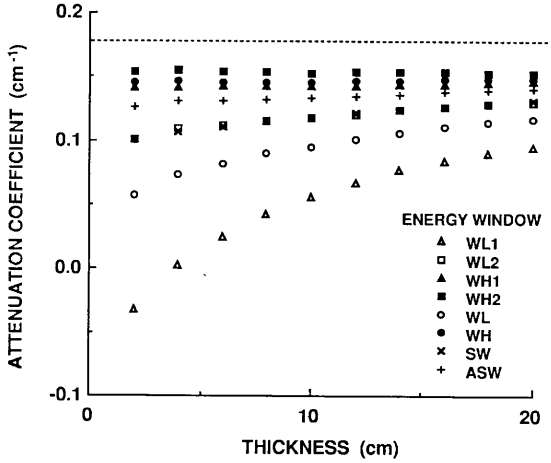

Fig. 6 Attenuation coefficients as a function of thickness for eight energy windows. The broken line shows the theoretical value (0.178 cm^{-1}).

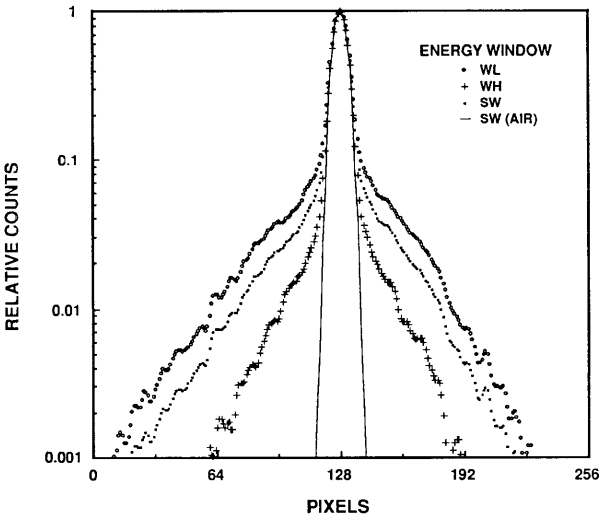

Fig. 7 Count profile curves of images acquired with three energy windows (WL, WH and SW) for a line source. The thickness of the forward scattering material was 10 cm. As a reference curve, the curve acquired by means of the SW in air was drawn.

Table 2 Average values of slope for right and left tales of LSF

	Energy window		
	WL	WH	SW
Slope (cm^{-1})	0.443	0.575	0.475

WL), the total counts within energy windows above 140 keV decreased linearly. Figure 5b shows that the scatter fractions for every window within the SW increased linearly as the thickness of the scattering material increased. The scatter fractions for every window above 140 keV are much smaller than those

for energy windows below 140 keV. Furthermore, from the scatter fractions for the WL and WH it could be seen that 75–80% of scattered photons in the SW are included in the WL. The use of the asymmetric energy window (ASW) can reduce the scatter fraction for the SW to about 2/3.

Figure 6 plots the attenuation coefficient against the thickness of the scattering material for all energy windows investigated. The attenuation coefficients for energy windows below 140 keV (WL1, WL2 and WL) showed greater variability and had smaller values than the theoretical value. However, for three energy windows above 140 keV (WH1, WH2 and WH), the attenuation coefficients were not affected by the thickness of the scattering material. In addition, although the values for these windows were closer to the theoretical one (0.178 cm^{-1}), there was an error of 14% for the WH2.

Profile curves for line source images acquired with three energy windows (WL, WH and SW) are shown in Fig. 7. As a reference image, a profile curve obtained in air was drawn together. The peak values for four curves were normalized to 1. It could be seen that the LSFs included scattered photons with tails which had nearly straight forms on semilogarithmic coordinates. This fact indicates that the tail of the LSF can be represented as a mono-exponential function. Then, we obtained the values for the slope for both tails of three LSFs and listed their average value in Table 2. The energy window WH had the largest value for the slope.

DISCUSSION

Scattered photons are included within a conventional symmetric energy window because of the finite energy resolution of a gamma camera.

A number of investigators have used a Monte Carlo simulation model for such an analysis of scattered photons. The Monte Carlo technique can discriminate scattered photons from non-scattered photons and depict energy and spatial distributions of scattered photons by means of a computer only. However, the Monte Carlo simulation has the following drawbacks: (1) time consuming for calculations; (2) demanding the validation of the Monte Carlo code by making a comparison with experimental measurements.

We quantitatively determined the amount of scattered photons in phantom experiments instead of with Monte Carlo calculations. Our results showed that scattered photons are distributed over the entire symmetric photopeak window (SW) and most of these scattered photons are included within the energy window below 140 keV (WL) (75–80%). From the detailed Monte Carlo studies it has been cleared that these events mainly consist of the first and second order Compton scattered photons.[1,2,6,7]

Many methods for correcting scattered photons have been developed.[3–5] The simpler methods employ the narrower symmetric energy window and the asymmetric energy window. Our results show that scattered photons can not be completely removed by any window selection.

It is important to consider backscattered photons in order to evaluate the scatter correction method which Jaszczak et al.[4] have proposed. We investigated the effect of backscattered photons with 10 cm backscattered material, which is thicker than the infinite thickness reported by Filipow et al.,[9] on a photopeak. As a result, it was seen that backscattered photons are distributed in energy regions below about 120 keV and do not affect the photopeak. Therefore, a scatter-window image used in the dual window method is influenced by not only multi-forward scattered photons but also such backscattered photons. This fact confirms that especially when a source is near the surface of a phantom, the normalized scatter-window image differs greatly from the true scatter image in the photopeak window.[10]

The spatial distribution of the first and second order Compton scattered photons is nearly mono-exponential in shape.[1,7] Our results also confirmed that the tails of LSFs obtained with three energy windows in the photopeak window have similar shapes. This characterization is available for scatter corrections which use either the convolution or deconvolution technique.[3,5]

We showed that the experimental measurements make possible quantitative analysis of scattered photons. Since the results of these studies can be applied to other phantom models, they may become useful in developing and evaluating a scatter correction method.

REFERENCES

1. Floyd CE, Jaszczak RJ, Harris CC, et al: Energy and spatial distribution of multiple order Compton scatter in SPECT: a Monte Carlo investigation. *Phys Med Biol* 29: 1217–1230, 1984
2. Floyd CE, Jaszczak RJ, Harris CC, et al: Revised scatter fraction results for SPECT. *Phys Med Biol* 32: 1663–1666, 1987
3. Axelsson B, Msaki P, Israelsson A: Subtraction of Compton-scattered photons in emission computed tomography. *J Nucl Med* 25: 490–494, 1984
4. Jaszczak RJ, Greer KL, Floyd CE, et al: Improved SPECT quantification using compensation for scattered photons. *J Nucl Med* 25: 893–900, 1984
5. Floyd CE, Jaszczak RJ, Greer KL, et al: Deconvolution of Compton scatter in SPECT. *J Nucl Med* 26: 403–408, 1985

6. Rosenthal MS, Henry LJ: Scattering in uniform media. *Phys Med Biol* 35: 265–274, 1990
7. Ogawa K, Harata Y, Ichihara T, et al: Estimation of scatter component in SPECT planar image using a Monte Carlo method. *Kaku Igaku* 27: 467–476, 1990
8. Hubbell JH: Photon cross sections, attenuation coefficients and energy absorption coefficients from 10 keV to 100 GeV. *Report NSRDS-NBS* 29, 1969
9. Filipow LJ, Macey DJ, Munro TR: The measurement of the depth of a point source of a radioisotope from gamma ray spectra. *Phys Med Biol* 24: 341–352, 1979
10. Ljungberg M, Msaki P, Strand SE: Comparison of dual-window and convolution scatter correction techniques using the Monte Carlo method. *Phys Med Biol* 35: 1099–1110, 1990